The Electronic Structures and Properties of Open-Ended and Capped Carbon Nanoneedles

Jenna L. Wang† and Paul G. Mezey*

Scientific Modeling and Simulation Laboratory (SMSL), Department of Chemistry and Department of Physics and Physical Oceanography, Memorial University of Newfoundland, St. John's, Newfoundland, Canada A1B 3X7

Received September 13, 2005

The existence of a family of very thin carbon needlelike nanostructures is predicted: the geometry and stability of several carbon nanoneedles (CNNs) formed by C_4 and C_6 units have been studied by quantum chemistry computational modeling methods. The structures of carbon nanoneedles are tighter than even the smallest single wall nanotubes (SWNTs) based on (4, 0) naphthacene. The electronic properties, energetic stability of geometrical structures with various terminal units are investigated. The relatively large band gaps, the strong bonding, and additional orbital interactions within the C_4 rings and between the C_4 layers make the $H_4(C_4)_nH_4$ type molecules nonmetallic. We have found indications that if the CNN (3, 0) structures are very long (in the limit of infinite-length), then they are likely to have semiconducting properties and could possibly be used as actual semiconductors. The studied families of CNNs can be considered as carbon nanostructures with unique structural and chemical properties and with possible potential for unusual electronic properties, with likely practical applications as nanomaterials and nanostructure devices.

I. INTRODUCTION

Theoretical and experimental research on carbon nanotubes (CNTs) are currently the focus of intense interest worldwide since their initial finding by Iijima in 1991.[1] The unique physical properties CNTs exhibit could have applications in broad areas of science and technology, ranging from exceptionally strong composites to nanoelectronics.[2−4]

After the discovery of single-walled carbon nanotubes (SWNTs) in 1993,[5,6] numerous applications have been found in chemistry and physics based on their anisotropic shapes, remarkable strengths, and elasticities as well as a wide range of unique electronic, optical, and mechanical properties.[7] Among the practical applications, their role in the collection and removal of toxic substances[8] and their uses as storage material for hydrogen,[9−11] nanoelectronic devices,[12,13] and building blocks with covalent functionalization[14] are significant. Theoretical calculations first predicted that SWNTs could exhibit either metallic or semiconducting behavior depending only on their diameter and helicity.[15−17] The ability to display fundamentally distinct electronic properties without essentially changing the local bonding, a fact that was recently experimentally demonstrated through scanning tunneling microscopy (STM) measurements of atomic resolution,[18,19] sets nanotubes apart from most other nanowire materials.[20,21] The early quantum-mechanical studies of SWNTs have been carried out using tight-binding model Hamiltonians[22−25] and all-electron semiempirical methods.[26] Electronic structures, energetics, and properties of SWNTs [5,5] and [9,0], are found to depend strongly on the tube length and, in the case of the [9,0] zigzag species, on the relative orientation of the caps.[27] Kawazoe and co-workers studied various structures of carbon and silicon nanotubes.[28−31] The shortest SWNTs, (4,0) naphthacene and (5,0) pentacene, were studied theoretically by Sun.[32] Most studies of SWNTs are focused on structures with diameter over 4 benzene rings.

By contrast, in this paper, a family of much more tightly packed carbon nanoneedles formed by units of C_4 and C_6 (3, 0) layers were investigated. Whereas one could possibly regard them as extreme cases of SWNTs, such classification can be misleading, since they are too tight to be called tubes and no other molecules can enter along the central axis of these structures; therefore, we refer to them as carbon nanoneedles (CNNs). The very thin structures cannot really function as actual tubes, so the nanoneedle expression is perhaps more appropriate.

Optimum geometrical structures, energetic stabilities, electronic structures, large scale electronic properties related to nonmetallic or semiconducting properties, and detailed energy relations of these carbon nanoneedles are studied theoretically.

II. COMPUTATIONAL METHODOLOGY

The optimized geometries and energetic stability were determined using the Gaussian 03 program[33] and the DFT method at B3LYP/6-31G* level.[34] For the verification and characterization of energy minima, harmonic vibrational frequency calculations were performed at the same level of theory. The computed energy values were corrected for zero-point energies. The binding energies (E_B) are calculated with respect to ground-state atoms contained in the investigated molecules, considering for instance the following formal dissociation reaction and the following equation for C_xH_y: $E_B = E_{CxHy} - (xE_C + yE_H)$. Standard heats of formation of nanoneedles $H_3(C_6)_nH_3$ (n=3−6) were calculated with refer-

* Corresponding author phone: (709)737-8768; fax: (709)737-3702, e-mail: paul.mezey@gmail.com.

† Present address: Molecular Graphic and Modelling Lab, University of Kansas.

10.1021/ci050402w CCC: $33.50 © 2006 American Chemical Society
Published on Web 02/21/2006

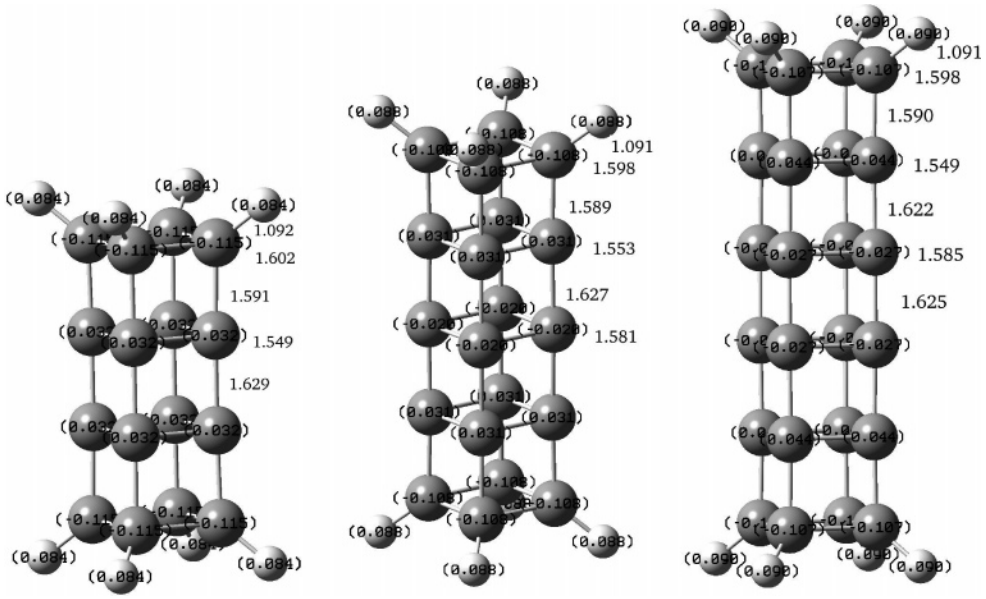

Figure 1. Bond-lengths and Mulliken charge distribution of poly-C_4 nanoneedles (D_{4h}) of 4 layers, 5 layers, and 6 layers.

ence to intermediate species and the following reaction: $H_3(C_6)_nH_3 + 2(n\text{-}1)CH_4 = (8n-2)/6\ C_6H_6$. The electron density distributions and the shapes of the electron density clouds in both the bonding regions and the peripheral regions of these nanoneedles were analyzed by the program Rhocalc 05 developed in our laboratory,[35] in order to elucidate some of the unusual but essential features of the bonding patterns.

III. RESULT AND DISCUSSIONS

Poly-C_4 nanoneedles (4−6 layers) were optimized to be characterized as minima by vibrational frequency calculation. The stable structures of zigzag poly-C_6 nanoneedles terminated by 3 oxygen atoms (2−10 layers), by 6 hydrogen atoms (3−5 layers), by 3 hydrogen atoms (3−6 layers), by 3 chlorine atoms (2−6 layers), and by capped C_3 (6, 7 layers) were also obtained and characterized to be minima by all real vibrational frequencies. Some optimum geometries and electronic charge distributions of two types of nanoneedles, formed by C_4 and C_6 layer units with different lengths and termination, respectively, are depicted in Figures 1−3. To study the energetic stability of CNNs, the calculation of standard heats of formation of nanoneedles $H_3(C_6)_nH_3$ (n=3−6) are shown in Table 1. $\Delta H°_{f1}$ can be expressed in terms of the increments of carbon atoms layers, $\Delta H°_{f1} = (8n-2)/6\Delta H°_{fC6H6} - 2(n-1)\Delta H°_{fCH4}$. It is obvious that the standard heats of formation of nanoneedle $H_3(C_6)_3H_3$ is higher than those of thicker nanostructures.

Nanoneedles of poly-C4 structures are also stable, at proper energy minima with all real vibrational frequencies. Bond-lengths and Mulliken charge distribution on poly-C_4 nanoneedles of the length of 4, 5, and 6 layers, with D_{4h} symmetry and terminated by hydrogen atoms, are described in Figure 1. There are slight differences of bond lengths (1.549−1.602 Å) and also in the charge distribution (H: 0.084−0.090e, C_{41}: −0.1e, C_{42}: 0.03e, C_{43}: 0.02e; here the notations C_{41}, C_{42}, and so on, refer to the first, second, etc. layer of the poly-C_4 nanoneedle). The layer-to-layer bond-lengths increase from the end layers to the center gradually becomes less noticeable when approaching the center; for instance, carbon−carbon bond-lengths between layers of $H_4(C_4)_nH_4$ (n=4−6) increase from 1.591→1.629 Å (n=4); 1.589 → 1.627 Å (n=5); and 1.590 → 1.622 → 1.625 Å (n=6).

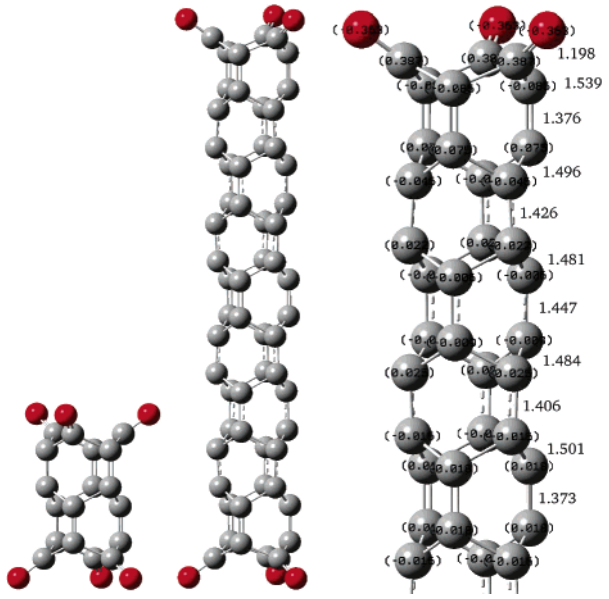

Figure 2. Open-ended poly-C_6 nanoneedles (D_{3d}): 3 layers, 10 layers, and the enlarged image of the top of 10 layers, terminated by oxygen atoms. The geometrical parameters and Mulliken charge distribution are indicated.

The electronic structure and chemical reactivity of armchair and zigzag type carbon nanotubes have been discussed in several studies.[36−40] Based on these studies, we find both analogies and differences with respect to the molecules studied in this work. The carbon−carbon bonds in molecule $H_4(C_4)_4H_4$ are stronger within layers than those between layers. The corresponding results for bond length are in agreement with the pattern of electron density contours shown in Figure 4(a). The weaker bonds between layers are indicated by isocontours which appear locally disconnected when the electron density isosurface with a threshold of 0.25 au (1 au for electron density = 1 e^-/bohr^3) is displayed, but at the same isodensity value the bonds within layers appear locally connected.

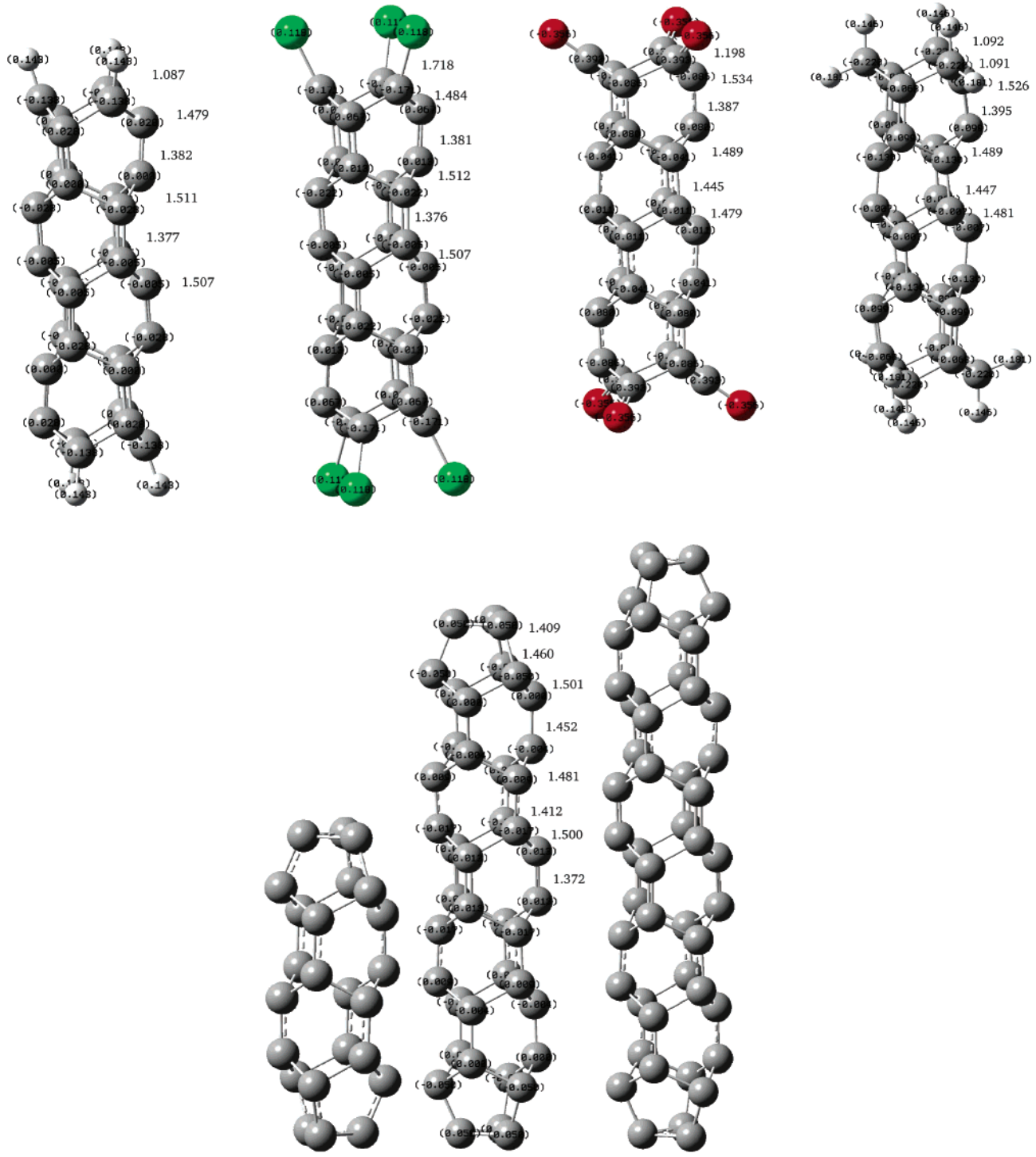

Figure 3. Open-ended poly-C_6 nanoneedles terminated by CH, CCl, CO, CH_2, and capped poly-C_6 nanoneedles terminated by C_3 triangles.

Table 1. Standard Heats of Formation of Nanoneedles $H_3(C_6)_nH_3$ (n=3−6)

$H_3(C_6)_nH_3$	$\Delta H°_{f1}$(kJ/mol)	$\Delta H°_f/n$ (kJ/mol)/n
$n = 3$	791.54	263.85
$n = 4$	2732.37	683.09
$n = 5$	3420.77	684.16
$n = 6$	4144.05	690.68

The extent of nonlocal features of HOMO and near-HOMO orbitals are often an indication of unusual electronic behavior. Figure 5a shows the orbital isosurfaces (isovalue=0.02 au) of the highest five occupied orbitals (HOMO → HOMO-4, two degenerate orbitals) and the lowest unoccupied (LUMO) molecular orbital of $H_4(C_4)_5H_4$. Some apparent conjugation seems to occur spanning two layers along the length of the nanoneedle, involving neighbor carbon atoms within ring layers (HOMO→ HOMO-3). The HOMO−LUMO energy gaps (3.4−3.6 eV) of the $H_4(C_4)_nH_4$ (n=4−6) nanoneedles are presented in Figure 6. The large band gaps and strong orbital overlaps both among layers and within layers confirm the expectation that the molecules $H_4(C_4)_nH_4$ have no metallic or semiconducting properties and are nonmetallic.

The CNNs (3, 0) $H_3(C_6)_nH_3$, $Cl_3(C_6)_nCl_3$, $O_3(C_6)_nO_3$, and $H_6(C_6)_nH_6$, terminated by H, O, and Cl atoms or capped by

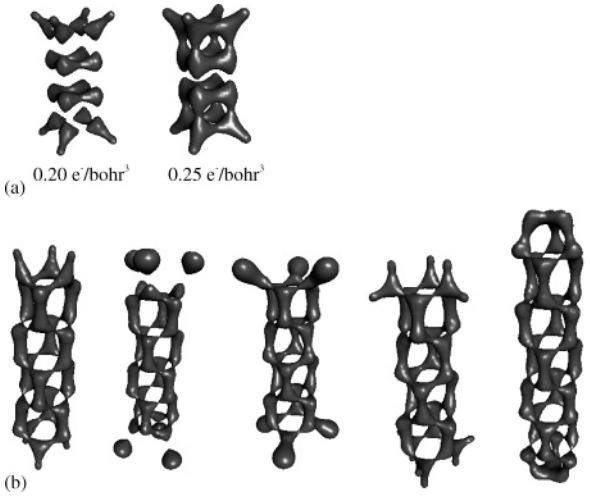

Figure 4. Electron densities of CNNs. (a) Selected isodensity contours of $H_4(C_4)_4H_4$. (b) Isodensity contours of poly-C_6 nanoneedles terminated by 3H, 3Cl, 3O, 6H, and $3C_3$ atoms (0.25 $e^-/bohr^3$).

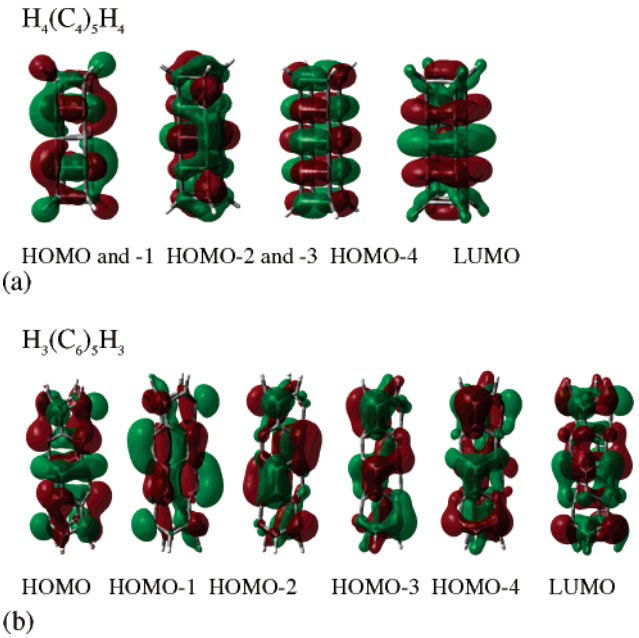

Figure 5. Patterns of some significant orbitals of CNNs. In part (a) the first two orbitals are degenerate.

C_3 triangles were investigated. The geometrical parameters are shown in Figures 2 and 3. Figure 2 also shows the geometries of nanoneedles of even layers with D_{3h} symmetry and odd layers with D_{3d} symmetry, where both types are terminated by oxygen atoms. The longest CNN minima in this work is formed by 10 layers of zigzag C_6 (D_{3d}) and terminated by oxygen atoms. Apparently, the charge distributions at the end layers show more negative charge, in part due to the presence of the electronegative oxygen atoms, and partly due to the general tendency of negative charge moving from the center to the periphery of molecules. The bond-lengths within layers are close to those of the usual C−C single bonds, whereas those between layers fall within the range between the average C═C double bond and C−C single bond.

Figure 3 shows five layers of poly-C_6 CNNs terminated alternatively by 3 H, 3 Cl, 3 O, and 6 H atoms. Here the differences of poly-C_6 CNNs terminated by different groups

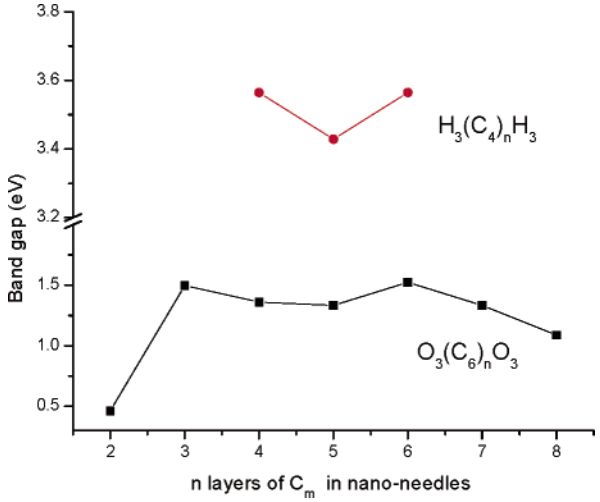

Figure 6. The energy gaps of *n* layer poly-C_4 nanoneedles.

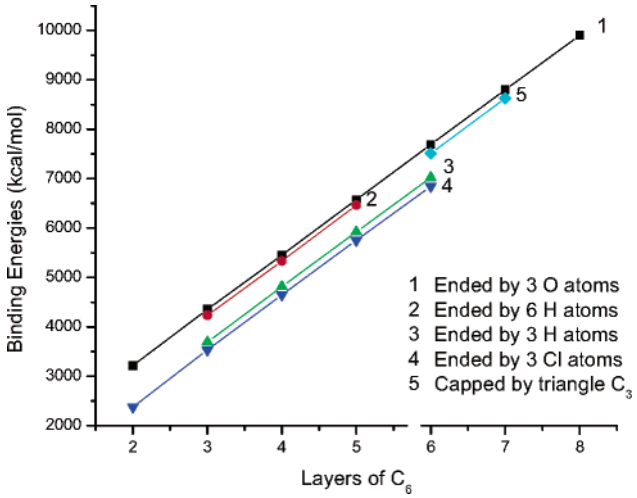

Figure 7. The total binding energies of *n* layer nanoneedles with unit layer C_6.

were investigated. In the cases of terminating C−H and C−Cl single bonds, the geometries of the inner layers change only very slightly, even though the electronegativities of the terminal atoms are rather different. Likewise, in the case of terminating groups CH_2 and C═O, both involving two terminating bonds, the corresponding inner layer carbon−carbon bonds change only slightly. However, between these two groups, the geometrical parameters of the carbon−carbon bonds within the inner regions of poly-C_6 CNNs show significant differences. For the capped CNNs, three examples of 3, 6, and 7 layers are shown in Figure 3. The Mulliken charge distribution in capped CNNs, especially for the terminal parts, is less polarized than in the other, open-ended CNNs. Consequently, the capped model more closely resembles the ideal, infinite-length poly-C_6 CNNs. However, the population analysis of electron density also shows some similar tendencies for open-ended and capped poly-C_6 CNNs. The bonds within layers are always weaker than those between layers (see Figure 4b); note that this result is fundamentally different from the result of the poly-C_4 CNNs $H_4(C_4)_nH_4$.

A qualitative orbital analysis of poly-C_6 CNNs also provides some insight, for instance, the HOMOs and LUMO of $H_3(C_6)_5H_3$ in Figure 5, strong delocalized bonding interactions occur not only around the layer of the C_6 rings

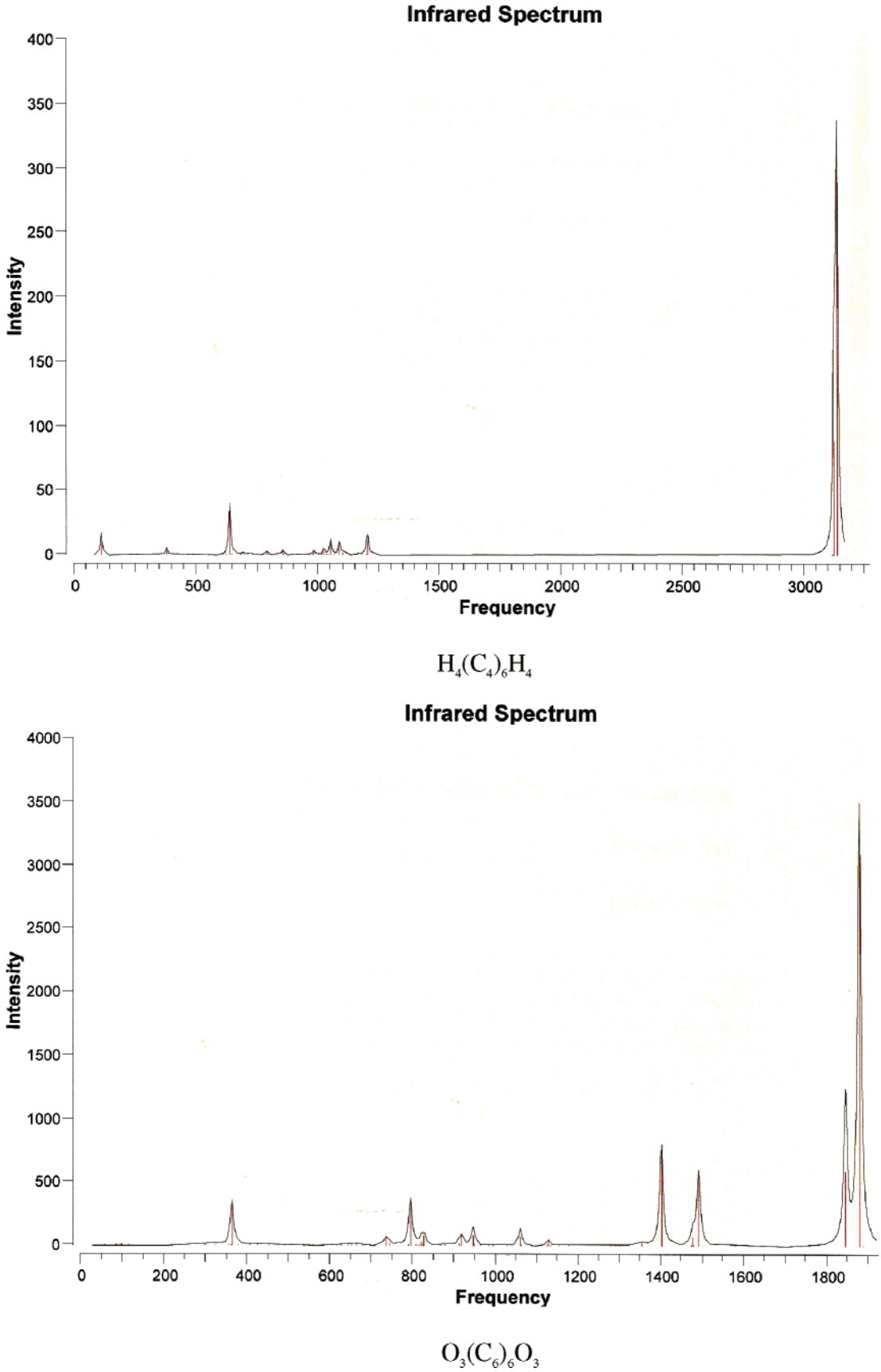

Figure 8. The computed infrared spectrum of $H_4(C_4)_6H_4$ and $O_3(C_6)_6O_3$.

(as shown by the HOMO) but also along the length of the needles through the HOMO-1 and by a different pattern between layers and along the needle length by the HOMO-3 and HOMO-4, respectively. In particular, HOMO-2 shows a strong delocalization along the needles. Not surprisingly, the qualitative conclusions obtained from the pattern of orbital isosurfaces agree well with those based on the electron density distributions.

The estimates of band gaps for the large n limit were obtained from the series involving two to eight layers of $O_3(C_6)_nO_3$ (see Figure 6). The calculated energy gaps fall within the range of 0.5−1.5 eV. The main tendency is a slight decrease, except for the energy gap of $O_3(C_6)_2O_3$, which is very special due to its short length, and the large number of C═O bonds.

All known experimental procedures for generating SWNTs give mixtures, according to nanotube lengths, diameters ($2R$), and chiralities. Following the usual characterization of carbon nanotubes by two integers, n and m, when $n - m = 0$, then the nanotube is metallic; when $n - m = 3q$, where q is an integer that does not equal 0, the nanotube is a small gap semiconductor with $E_{gap} \propto 1/R^2$; and other tubes have larger gaps proportional to $1/R$. The result we obtained for nanoneedles can be compared with the results of HOMO and LUMO energies of [9, 0] zigzag SWNTs capped with C_{30} hemispheres in ref 27 which was obtained theoretically and agrees well with the experimental data.[40] The band gaps become smaller with the increasing length of [9, 0] zigzag SWNTs (from one layer of 2.45 eV to eight layers of 0.84 eV). An infinite-length [9,0] zigzag SWNT is predicted to be a semiconductor rather than a metal, irrespective of the presence of caps. It is known that stability increases with the increase of the diameter of SWNTs. In our case, the total binding energies (E_b) of n layers with unit layers C_6 are presented in Figure 7. The gradient of E_b is nearly constant with increasing n for each different terminal group; that is, the bond forming tendency does not change much with length, and very long (quasi infinite-length) CNNs could exist theoretically. The E_b value of $O_3(C_6)_{10}O_3$ was obtained as 1.08 eV, representing a small change when compared to that of $O_3(C_6)_8O_3$. Although we have actually calculated structures and electronic properties of CNNs only up to 10 layers, from the tendency of energy gaps, we conclude that infinite-length CNNs (3,0) are likely to have semiconducting properties, and very long CNNs (3,0) could possibly be used as semiconductors in nanostructure devices.

The theoretical infrared (IR) spectra of $H_4(C_4)_6H_4$ and $O_3(C_6)_6O_3$ are given as examples in Figure 8. Potentially, their IR spectra could indicate the different bonding characters of carbon−carbon bonds in these two different CNN structures.

For the IR spectrum of $H_4(C_4)_6H_4$, the strong peak at 3130 cm^{-1} may be assigned to the vibration of C−H bonds. Around 640 and 1200 cm^{-1}, there are weak signals from C−C vibrations within layers in the middle of CNNs and the two terminating rings, respectively. Around 975 to 1100 cm^{-1}, there is a group of very weak signals from C−C bond vibrations between layers. There is no apparent signal for "C═C" vibrations in the IR of $H_4(C_4)_6H_4$. For the IR spectrum of $O_3(C_6)_{10}O_3$, the vibrations of the C═O bonds give strong signals at 1850 and 1889 cm^{-1}. At 1402 cm^{-1} and 1493 cm^{-1}, the signals can be assigned to the vibrations of C═C bonds between layers in the middle layers and end layers of CNNs, respectively. The signal at 1063 cm^{-1} is that of the C−C vibration within layers only from the middle layers of CNNs. The signals at 355 cm^{-1} to 960 cm^{-1} are apparently from the vibrations of C−C bonds within rings of the CNNs. These results and their interpretation are in good agreement with the electron density and orbital analysis of the electronic structures.

IV. SUMMARY

The geometries and electronic properties of the structures of the tight carbon nanoneedles, poly-C_4 CNNs and poly-C_6 CNNs, have been computed and analyzed at the B3LYP/6-31G* level. The energy per carbon of CNNs, of course, is quite high when compared to well-known carbon structures, such as graphite, diamond, or C_{60}. The computed properties of the molecule $H_4(C_4)_nH_4$ indicate that for large n they have a nonmetallic character. The ideal, infinite-length poly-C_6 CNNs, CNNs (3, 0) are likely to be semiconductors, irrespective of the ending groups, and they could be useful as semiconductors in nanostructure devices. It might also be possible to synthesize one-dimensional polymeric wires of these materials.

Compared with normal carbon nanotubes, the CNNs are extremely tight carbon nanostructures which may possess significant strain energy resulting from structure distortion. Therefore, the potentially useful role of large strain energy in some applications and possible structure modifications for circumventing such strains concerning the subject of the energetic stability of CNNs have been considered for additional studies in our future work.

ACKNOWLEDGMENT

This study has been supported by the Natural Sciences and Engineering Research Council of Canada.

REFERENCES AND NOTES

(1) Iijima, S. Helical microtubules of graphitic carbon. *Nature* **1991**, *354*, 56−58.
(2) Dresselhaus, M. S.; Dresselhaus, G.; Eklund, P. C. *Science of Fullerenes and Carbon Nanotubes*; Academic: San Diego, 1996.
(3) Dekker: C. Carbon nanotubes as molecular quantum wires. *Phys. Today* **1999**, *52*, 22.
(4) Ouyang, M.; Huang, J.-L.; Lieber, C. M. Fundamental electronic properties and applications of single-walled carbon nanotubes. *Acc. Chem. Res.* **2002**, *35*, 1018−1025.
(5) Iijima, S.; Ichihashi, T. Single-shell carbon nanotubes of 1-nm diameter. *Nature* **1993**, *363*, 603−605.
(6) Bethune, D. S.; Kiang, C. H.; Vries, M. S. de; Gorman, G.; Savoy, R.; Vazquez, J.; Bevers, R. Cobalt-catalysed growth of carbon nanotubes with single-atomic-layer walls. *Nature* **1993**, *363*, 605−607.
(7) Ajayan, P. M. Nanotubes from Carbon. *Chem. Rev.* **1999**, *99*, 1787−1800.
(8) Long, R. Q.; Yang, R. T. Carbon Nanotubes as Superior Sorbent for Dioxin Removal. *J. Am. Chem. Soc.* **2001**, *123*, 2058−2060.
(9) Lee, S. M.; An, K. H.; Lee, Y. H.; Seifert, G.; Frauenheim, T. A Hydrogen Storage Mechanism in Single-Walled Carbon Nanotubes. *J. Am. Chem. Soc.* **2001**, *123*, 5059−5060.
(10) Froudakis, G. E. Hydrogen interaction with carbon nanotubes: a review of ab initio studies. *J. Phys.: Condens. Matter* **2002**, *14*, R453−R465.
(11) Dillon, A. C.; Jones, K. M.; Bekkedahl, T. A.; Kiang, C. H.; Bethune, D. S.; Heben, M. J. Storage of hydrogen in single-walled carbon nanotubes. *Nature* **1997**, *386*, 377−379.
(12) McEuen, P. Nanotechnology: Carbon-based electronics. *Nature* **1998**, *393*, 15−17.
(13) Nojeh, A.; Lakatos, G. W.; Peng, S.; Cho, K.; Fabian, R. A carbon nanotube cross structure as a nanoscale quantum Device. *Nano Lett.* **2003**, *3*, 1187−1190.
(14) Saito, R.; Dresselhaus, G.; Dresselhaus, M. S. *Physical Properties of Carbon Nanotubes*; Imperial College Press: London, 1998.
(15) Hamada, N.; Sawada, S.; Oshiyama, A. New one-dimensional conductors: Graphitic microtubules *Phys. Rev. Lett.* **1992**, *68*, 1579−1581.
(16) Mintmire, J. W.; Dunlap, B. I.; White, C. T. Are fullerene tubules metallic? *Phys. Rev. Lett.* **1992**, *68*, 631−633.
(17) Saito, R.; Fujita, M.; Dresselhaus, G.; Dresselhaus, M. S. Electronic structure of chiral graphene tubules. *Appl. Phys. Lett.* **1992**, *60*, 2204−2206.

(18) Wildoer, J. W. G.; Venema, L. C.; Rinzler, A. G.; Smalley, R. E.; Dekker, C. Electronic structure of atomically resolved carbon nanotubes. *Nature* **1998**, *391*, 59−61.
(19) Odom, T. W.; Huang, J.-L.; Kim, P.; Lieber, C. M. Atomic structure and electronic properties of single-walled carbon nanotubes. *Nature* **1998**, *391*, 62−64.
(20) Lieber, C. M. One-dimensional nanostructures: Chemistry, physics & applications. *Solid State Comm.* **1998**, *107*, 607−616.
(21) Hu, J.; Odom, T. W.; Lieber, C. M. Chemistry and Physics in One-Dimension: Synthesis and Properties of Nanowires and Nanotubes. *Acc. Chem. Res.* **1999**, *32*, 435−445.
(22) Kane, C. L.; Mele, E. J. Size, shape, and low energy electronic structure of carbon nanotubes *Phys. Rev. Lett.* **1997**, *78*, 1932−1934.
(23) Ma, J.; Yuan, R. K. Electronic and optical properties of finite zigzag carbon nanotubes with and without Coulomb interaction. *Phys. Rev. B* **1998**, *57*, 9343−9348.
(24) Jiang, J.; Dong, J.; Xing, D. Y. Size and helical symmetry effects on the nonlinear optical properties of chiral carbon nanotubes. *Phys. Rev. B* **1999**, *59*, 9838−9841.
(25) Liang, W. Z.; Yokojima, S.; Zhou, D. H.; Chen, G. H. Localized-Density-Matrix Method and Its Application to Carbon Nanotubes. *J. Phys. Chem. A* **2000**, *104*, 2445−2453.
(26) Liang, W. Z.; Yokojima, S.; Ng, M. F.; Chen, G. H.; He, G. Optical Properties of Single-Walled 4 Å Carbon Nanotubes. *J. Am. Chem. Soc.* **2001**, *123*, 9830−9831.
(27) Cioslowski, J.; Rao, N.; Moncrieff, D. Electronic structures and energetics of [5,5] and [9,0] single-walled carbon nanotubes. *J. Am. Chem. Soc.* **2002**, *124*, 8485−8486.
(28) Singh, A. K.; Briere, T. M.; Kumar, V.; Kawazoe, Y. Magnetism in transition-metal-doped silicon nanotubes *Phys. Rev. Lett.* **2003**, *91*, 146802−146805.
(29) Kumar, V., Kawazoe, Y. Hydrogenated silicon fullerenes: Effects of H on the stability of metal-encapsulated silicon clusters. *Phys. Rev. Lett*. **2003**, *90*, 55502−55505.
(30) Singh, A. K. Kumar, V. Briere, T. M., Kawazoe, Y. Cluster assembled metal encapsulated thin nanotubes of silicon. *Nano Lett*. **2002**, *2*, 1243−1248.
(31) Singh, A. K.; Kumar, V.; Kawazoe, Y. Structure of the thinnest most stable semiconducting and insulating nanotubes of SiO_x (x=1,2). *Phys. Rev. B* **2005**, *72*, 155422−155426.
(32) Sun, C. H.; Finnerty, J. J.; Lu, G. Q.; Cheng, H. M. Stability of Supershort Single-Walled Carbon Nanotubes. *J. Phys. Chem. B* **2005**, *109*, 12406−12409.
(33) Frisch, M. J.; Trucks, G. W.; Schlegel, H. B.; Scuseria, G. E.; Robb, M. A.; Cheeseman, J. R.; Montgomery, J. A., Jr.; Vreven, T.; Kudin, K. N.; Burant, J. C.; Millam, J. M.; Iyengar, S. S.; Tomasi, J.; Barone, V.; Mennucci, B.; Cossi, M.; Scalmani, G.; Rega, N.; Petersson, G. A.; Nakatsuji, H.; Hada, M.; Ehara, M.; Toyota, K.; Fukuda, R.; Hasegawa, J.; Ishida, M.; Nakajima, T.; Honda, Y.; Kitao, O.; Nakai, H.; Klene, M.; Li, X.; Knox, J. E.; Hratchian, H. P.; Cross, J. B.; Bakken, V.; Adamo, C.; Jaramillo, J.; Gomperts, R.; Stratmann, R. E.; Yazyev, O.; Austin, A. J.; Cammi, R.; Pomelli, C.; Ochterski, J. W.; Ayala, P. Y.; Morokuma, K.; Voth, G. A.; Salvador, P.; Dannenberg, J. J.; Zakrzewski, V. G.; Dapprich, S.; Daniels, A. D.; Strain, M. C.; Farkas, O.; Malick, D. K.; Rabuck, A. D.; Raghavachari, K.; Foresman, J. B.; Ortiz, J. V.; Cui, Q.; Baboul, A. G.; Clifford, S.; Cioslowski, J.; Stefanov, B. B.; Liu, G.; Liashenko, A.; Piskorz, P.; Komaromi, I.; Martin, R. L.; Fox, D. J.; Keith, T.; Al-Laham, M. A.; Peng, C. Y.; Nanayakkara, A.; Challacombe, M.; Gill, P. M. W.; Johnson, B.; Chen, W.; Wong, M. W.; Gonzalez, C.; and Pople, J. A. *Gaussian 03, Revision C.02*; Gaussian, Inc.: Wallingford, CT, 2004.
(34) Becke, A. D. *J. Chem. Phys*. **1993**, *98*, 5648−5652. (b) Lee, C.; Yang, W. Parr,; R. G. Development of the Colle-Salvetti correlation-energy formula into a functional of the electron density. *Phys. Rev. B* **1988**, *37*, 785−789.
(35) Walker, P. D.; Warburton, P.; Wang, L. J.; Mezey, P. G. *Rhocalc*, *version05*; St. John's, NL A1B 3X7, 2005.
(36) Joselevich, E. Electronic Structure and Chemical Reactivity of Carbon Nanotubes. *ChemPhysChem* **2004**, 5, 619−624.
(37) Tanaka, K.; Okahara, K.; Okada, M.; Yamaba, T. Electronic properties of bucky-tube model. *Chem. Phys. Lett.* **1992**, *191*, 469−472.
(38) Lukovits, I.; Janežič, D. Enumeration of conjugated circuits in nanotubes. *J. Chem. Inf. Comput. Sci.* **2004**, *44*, 410−414.
(39) White, C. T.; Robertson, D. H.; Mintmire, J. W. Helical and rotational symmetries of nanoscale graphitic tubules. *Phys. Rev. B* **1993**, *47*, 5485−5488.
(40) Ouyang, M.; Huang, J. L.; Cheung, C. L.; Lieber, C. M. Energy gaps in "metallic" single-walled carbon nanotubes. *Science* **2001**, *292*, 702−705.

CI050402W